

# Towards Automated Breast Mass Classification using Deep Learning Framework

Pinaki Ranjan Sarkar\*, Priya Prabhakar\*, Deepak Mishra\*

\* Department of Avionics

IIST, Thiruvananthapuram, India-695547

(sarkar0499pinaki, priya8695, vr.dkmishra)@gmail.com

Gorthi R.K.S.S. Manyam

Department of Electrical Engineering

IIT Tirupati, India-517506

rkg@iittp.ac.in

**Abstract**—Due to high variability in shape, structure and occurrence; the non-palpable breast masses are often missed by the experienced radiologists. To aid them with more accurate identification, computer-aided detection (CAD) systems are widely used. Most of the developed CAD systems use complex handcrafted features which introduce difficulties for further improvement in performance. Deep or high-level features extracted using deep learning models already have proven its superiority over the low or middle-level handcrafted features. In this paper, we propose an automated deep CAD system performing both the functions: mass detection and classification. Our proposed framework is composed of three cascaded structures: suspicious region identification, mass/no-mass detection and mass classification. To detect the suspicious regions in a breast mammogram, we have used a deep hierarchical mass prediction network. Then we take a decision on whether the predicted lesions contain any abnormal masses using CNN high-level features from the augmented intensity and wavelet features. Afterwards, the mass classification is carried out only for abnormal cases with the same CNN structure. The whole process of breast mass classification including the extraction of wavelet features is automated in this work. We have tested our proposed model on widely used DDSM and INbreast databases in which mass prediction network has achieved the sensitivity of 0.94 and 0.96 followed by a mass/no-mass detection with the area under the curve (AUC) of 0.9976 and 0.9922 respectively on receiver operating characteristic (ROC) curve. Finally, the classification network has obtained an accuracy of 98.05% in DDSM and 98.14% in INbreast database which we believe is the best reported so far.

**Index Terms**—computer-aided detection, mammogram, convolutional neural network, wavelet transform, high-level features

## I. INTRODUCTION

Breast cancer is the most diagnosed deadly disease among women and the second leading cause of death [1]. In 2012 nearly 48.45% breast cancer patients died in India [2]. However, the five-year survival rate of early stage breast cancer is around 90% and its early detection can increase patients' survivability. Mammography is the most popular and reliable imaging modality [3] for breast cancer detection. Diagnosing the mammograms is a very challenging task even for experienced radiologists due to the non-palpable structures of breast masses. So, computer-aided detection (CAD) can be used to assist radiologists for the early detection of breast cancer. The primary objective of the CAD system is to detect the cancerous cells with a low false negative rate [4]. Detection

of masses is a herculean task due to the variation in intensity, size and appearance of masses in mammograms. Correct diagnose necessitates the successful detection of masses. Most of the detected masses are prone to be benign and therefore, the classification as benign or malignant is crucial. Benign tumours are not life-threatening unless they are pressing some blood vessels or tissues. On the other hand, malignant tumours are comprised of cancerous cells and if their detection is too late, it may spread imminently throughout the body with the less survival chance. In order to develop an automated CAD system, we have proposed a framework for both mass detection and its classification. To detect the suspicious lesions in mammograms we have used a Fully Convolutional Deep Hierarchy Saliency Network (FCDHSNet) which is a modified version of the DHS-Network proposed by Liu *et al.* [5]. We have made the network fully convolutional which reduces the number of trainable parameters. The proposed model provides a probabilistic map highlighting the region of interest. The incorporation of CNN with recurrent convolutional neural network extracts the felicitous features instead of depending upon a certain set of handcrafted features. To reduce the false positives, we have used a convolutional neural network in conjunction with two-dimensional discrete wavelet features for the classification of detected lesions as mass or no-mass. After detecting the possible abnormal regions from the prediction map, a pre-trained CNN model on mass/no-mass classification is fine-tuned for benign or malignant mass classification task.

The rest of the paper is organized as follows: in the Related works subsection, the existing works and the motivation for this paper are discussed. Proposed Methodology section covers the full framework of our proposed network in detail. The database along with the experiments done in this paper are discussed in the Experiments and Results section. Discussion section highlights the obtained results and its comparison with the state-of-the-art. We make our final remarks in Conclusion and Future works.

### A. Related works

Recently the Deep learning paradigm is proven to be one of the best approaches for computer vision, machine learning and speech processing etc. as it is very good at learning intricate structures in high-dimensional data [6]. Recent works using deep learning have shown better performance on breast tissue

classification. Ertosun *et al.* proposed a method in which two CNNs are used for breast mass detection and achieved the sensitivity of 0.85 [7]. Hu *et al.* proposed a method which integrates visual saliency with deep learning techniques [8]. Dhungel *et al.* proposed a mass detection technique which is based on multi-scale deep belief nets and Gaussian mixture model followed by a false positives reduction step using CNN and a random forest classifier [9]. Bayesian optimization is done on the selected hypothesis and their detection model shows 90% accuracy at 1 false positive per image.

To classify masses as benign or malignant, many authors have used deep learning frameworks and achieved good accuracy. Atlas *et al.* proposed to use the fusion of the most relevant morphological features for the classification of mass as benign or malignant [10]. Their method achieved 97.5% accuracy with the artificial neural network as the classifier. Arevalo *et al.* used CNN to extract features from mammograms and applied support vector machine (SVM) for the classification task [11]. Jiao *et al.* has extracted mid-level features i.e., shape, size etc. from the last convolutional layer of their proposed network and high-level features (it is extracted from the fully connected layer of the network) from mammograms and fused them for better simulating the real diagnostic process. Then the classification task is carried out by SVM classifiers in a two-step decision mechanism [12]. P.R.Sarkar et al. has used CNN as feature extractor as well as classifier and achieved 99.267% recognition accuracy in DDSM database [13]. The deep features are extracted from the ROIs in this work. Most of the techniques discussed in the literature focused either on the detection of masses or the classification. There are few works on end-to-end automated CAD system with satisfactory performance. In [9], [14] authors have proposed a hybrid CAD system with a combination of handcrafted features and deep features extracted from ROIs. Papers like [15], [16] have demonstrated the effectiveness of YOLO based CAD system [17].

Most of the non-Deep Learning (DL) papers relied upon a certain set of features which put a limit to their obtained results. Due to high variability in structure, size and occurrence of mass, extracting only a certain set of features like shape, size limit their result. They used multiple features to achieve good performance. The above mentioned techniques are mostly based on low or middle-level features which put a limit to either mass detection or mass classification problem. Inspired by the promising results achieved by [9], [14]–[16], [18], we propose to use a fully automated CAD system. We break the whole system in three stages: suspicious region identification, mass/no-mass detection and malignant/benign mass classification. Our approach for detection is similar to that of Hu *et al.* [8] but proved to be a better model with lower false positives per image. We have used CNN which automatically learns an optimal combination of various characteristics of mass and outputs a prediction map. We observe that deep features from contrast enhanced images performed better than the traditional detectors. Deep features enable the network to learn the aspects of the input which are important

for discrimination while suppressing the irrelevant variations [6]. The classification uses semantic/abstract features extracted from wavelet decomposed images as this allows to use both the spectral and spatial features. This fusion technique outperforms state-of-the-art classification performances. Our contributions in this paper are the following:

- we propose to use a fully convolutional deep hierarchical saliency prediction network to detect suspicious regions in a mammogram. In this stage, we treat the masses as salient objects in breast and learn the optimal combination of different salient cues for detection.
- we have shown that using both the spectral and spatial features leads to better classification performance compared to the other CNN techniques which usually learn only from the raw input pixels.
- we take the benefit of transfer learning [19] during our experiments. Most of the CAD systems using deep learning suffer from the lack of training data. Our pre-trained model on augmented DDSM database was fine-tuned on smaller database i.e., INbreast and it has shown impressive results in all the stages of the automated framework.

## II. PROPOSED METHODOLOGY

Due to low signal-to-noise ratio (SNR) and background artifacts, we need to segment the breast regions from the mammogram. We segmented breast regions from the mammograms using multilevel hierarchical thresholding and removed the pectoral masses using region growing segmentation method as the initial pre-processing step. Our proposed automated framework has three stages as shown in Fig.1: suspicious region identification, mass/no-mass detection and mass classification. In the subsequent subsections, we will present detailed description of each stage.

### A. Suspicious region identification

In the present diagnosis process, radiologists first identify suspicious lesions. Then, radiologists used the knowledge and awareness obtained with previous experience in a similar task (analogous to trained network in DL) to make the judgment of whether the suspicious lesion is a benign or malignant [12]. Inspired by the diagnostic process, we propose a fully convolutional deep hierarchical saliency network (FCDHSNet) for detecting suspicious regions in breast mammograms. FCDHSNet is an improved version of the DHSNet proposed by Liu *et al.* [5]. The network was originally developed to serve the purpose of salient object detection predicts a probability map of suspicious regions from the high-level features which are learned during training. Considering masses as salient objects, we have used it to detect suspicious regions from the mammograms. Our proposed FCDHSNet initially detects salient objects coarsely from a global view (like taking a glance from mammogram). This coarse prediction network predicts a coarse probability map of suspicious regions from the high-level features which are learned during training. Then, the probability map is further refined by a hierarchical

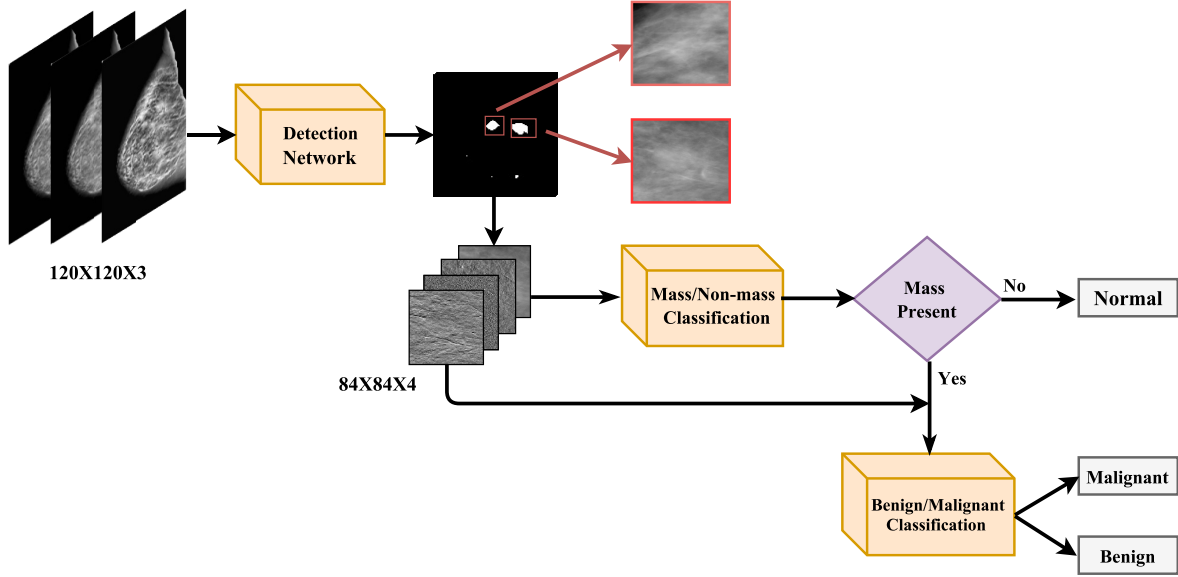


Fig. 1: Proposed automated breast mass classification network.

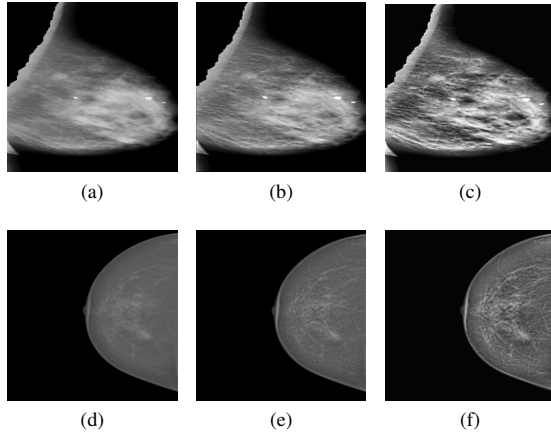


Fig. 2: (a) (d) Original mammogram (b) (e) Multi-scale top-hat transformed mammogram (c) (f) Enhanced mammogram using contrast limited histogram equalization. (a - c) images are from DDSM & (d - f) are from INbreast database.

recurrent convolutional neural network (HRCNN). HRCNN hierarchically and progressively improves the image details by integrating local contexts which is similar to the hierarchical impression of mass images and information processing of experts' brain (like the knowledge and experience gained from similar tasks) by using local contextual information to transform the coarse prediction probability map to a refined prediction map. We will now discuss the stages of mass detection network: preprocessing of the mammograms, coarse detection network and finer detection network.

**Preprocessing:** Efficient contrast enhancement in mammograms improves the detection performance as well as the clas-

sification accuracy [20], [21]. While doing several experiments with the FCDHSNet, we found that the network performs better when we train the network with differently contrast enhanced mammograms. The structure of the input image fed to the FCDHSNet is given below:

$input[:, :, 1]$  = original mammogram

$input[:, :, 2]$  = multi-scale top-hat transformed mammogram

$input[:, :, 3]$  = CLAHEd mammogram

where contrast limited adaptive histogram equalized mammogram [22] is written as CLAHEd. This is the improved version of histogram equalization where whole image is divided into small patches and each patch's histogram matches with the desired histogram. This adaptive histogram equalization may result in the amplification of noise and therefore, it is thresholded to limit the contrast enhancement induced by this method to a user selectable maximum. The 3 channel input image with CLAHEd enhancement will have high intensity at the dense and at the fatty locations which will help the detection network to combine optimal parameters to predict suspicious regions. In the second channel, we have used multi-scale top-hat transform based algorithm for enhancement, proposed by Bai *et al.* [23]. This neutralizes the over enhancement done by CLAHEd method. Sample images after preprocessing are shown in Fig.2.

**Coarse detection network:** DHSNet proposed by Liu *et al.* [5] is composed of coarse detection network and finer detection network. They have used VGG16 network [24] for the coarse detection. Due to the large network size of VGG16, computation of one epoch required nearly 180 minutes in our system (Intel®Xeon, 3.07GHz CPU with 24GB RAM and graphics card NVIDIA Quadro 6000 6144 MB GDDR5). So, in-order to reduce the computation time without affecting the

performance, we have used a modified VGG16 network with its fully connected layer replaced by a convolutional layer. This modification leads to the computation time of only 30 minutes for one epoch with reduction of trainable parameters from 10 million to 0.3 million. Replacement of fully connected layer with a convolutional layer also gives the advantage of spatial information that fully connected layer lacks as all the output neurons are connected to each of the input neurons. This is done by convolving the feature maps at 13<sup>th</sup> layer with a kernel of size  $1 \times 1$ . The network architecture is shown in Fig. 3. The network outputs a coarse prediction map which has higher values at the abnormal regions but it fails in detecting the subtle structures and preserving the local details. The reason is that four max-pooling layers in the VGG16 abandoned some spatial information and reduce the size of the original mammograms by a factor of 8. As a result, the subtle structures are missing from the prediction output. However, recurrent convolutional layer (RCL) is used for hierarchical and progressive refinement of the coarse prediction map.

*Finer detection network:* The key module of the finer prediction network is the recurrent convolutional layer (RCL). RCL enhances the quality of prediction map by evolving its states over discrete time steps. A RCL with  $[n]$  time steps can be unfolded to  $[n + 1]$  feed-forward networks and in our case  $n = 4$ . Each unfolded RCL has several paths of different depths from input to the output. The combination of these paths makes it less prone to over-fitting. The feedback connection of output with input helps to incorporate the local context efficiently. Feature learning is better due to the presence of context information which is provided by the feedback connection. Due to this, the RCL block helps in refining the output obtained from the coarse output network. For more detailed explanation refer [25].

The three channel input as discussed above of size  $120 \times 120$  is fed to the coarse detection network. The output of the coarse detection network is merged with conv 4\_3 layer output and then fed to a RCL block. The RCL block is fed with the obtained output merged with conv 3\_2 layer output. The obtained output is upsampled and merged with conv 2\_2 layer output followed by a RCL block. The output of this layer is of the same size as of the input data and merged with conv 1\_2 layer output. Before merging hidden layer output with RCL, it is passed through a convolutional layer with  $96 \ 1 \times 1$  convolutional kernels and sigmoid activation function to squash the features of the VGG16 layer. This decreases the number of feature maps of the VGG16 layer to save computational cost and we squash the range of the activation values of the neurons within  $[0, 1]$  by using sigmoid activation function. Without doing this, the combined prediction map will be overwhelmed with ReLU activation values in each layer of the VGG16 network. To facilitate learning, we resized the ground truths and saliency masks to sizes 120 and 60 for supervising the corresponding learning of each suspicious region.

*Training of FCDHSNet:* Backpropagation algorithm is applied to update the parameters during training in conjunction

with *Stochastic Gradient Descent* (SGD) optimization procedure. We define a loss function which quantifies the pixel-wise similarity between the ground truth and predicted map. The overall loss function, we used is described below:

$$\text{Loss} = ||\phi(\text{input}_i) - t||^2$$

where  $\phi(\text{input}_i)$  is the predicted map and  $t$  is the ground truth. The optimization technique finds out the way to update the network parameters which minimises the loss function. The learning rate and momentum parameters during training stage were initialized at 0.001 and 0.85 respectively. Learning rate was divided by 10 when the f-measure stopped improving with the current learning rate.

### B. Mass/no-mass detection

After acquiring the prediction map of the suspicious regions, we segmented each region automatically using centROID information. To minimize the loss of information prediction map is upsampled to  $1024 \times 1024$ . The prediction map contains abnormal masses and dense tissues as well. To predict the mass in the predicted map, we trained another convolutional neural network by providing intensity and wavelet features together as inputs to the network. The method used in this paper is motivated by Jadoon *et al.* [26]. But in this paper, we used two dimensional discrete wavelet transform to extract descriptive features. This provides spatial and spectral features to the network which helps to extract higher level features from both these complementary information. The architecture of the proposed CNN and the need for incorporation of wavelet features is discussed below.

*Spectral features extraction:* After segmenting the ROIs, we perform *Daubechis wavelet transform* [27] (db-4) on each ROI (let, one ROI is denoted as  $f_{2^{j+1}}$ ). The discrete wavelet transform decomposes the pre-segmented mammogram ROIs into four sub-images in different resolution levels preserving the high and low frequency resolution. Mathematically, we can represent the transformation as:

$$f_{2^{j+1}} = c_{2^j}^h + c_{2^j}^v + c_{2^j}^d + f_{2^j}^a \quad (1)$$

where,  $f_{2^{j+1}}$  is the input ROI at  $2^{j+1}$  resolution and  $c_{2^j}^h, c_{2^j}^v, c_{2^j}^d, f_{2^j}^a$  are the sub-images in horizontal, vertical, diagonal direction and approximated ROI at  $2^j$  resolution, respectively. The decomposed sub-images are the representative of two dimensional orthogonal wavelets.

*Training of CNN network:* We train the proposed CNN network with normalized sub-images along with the normalized ROIs. The structure of the input is given below:

$$\begin{aligned} \text{input}[:, :, 1] &= c_{2^j}^h \\ \text{input}[:, :, 2] &= c_{2^j}^v \\ \text{input}[:, :, 3] &= c_{2^j}^d \\ \text{input}[:, :, 4] &= f_{2^j}^a \end{aligned}$$

4 convolutional layers are used in our network followed by 4 max-pooling layers as described in Table II. We have used 2

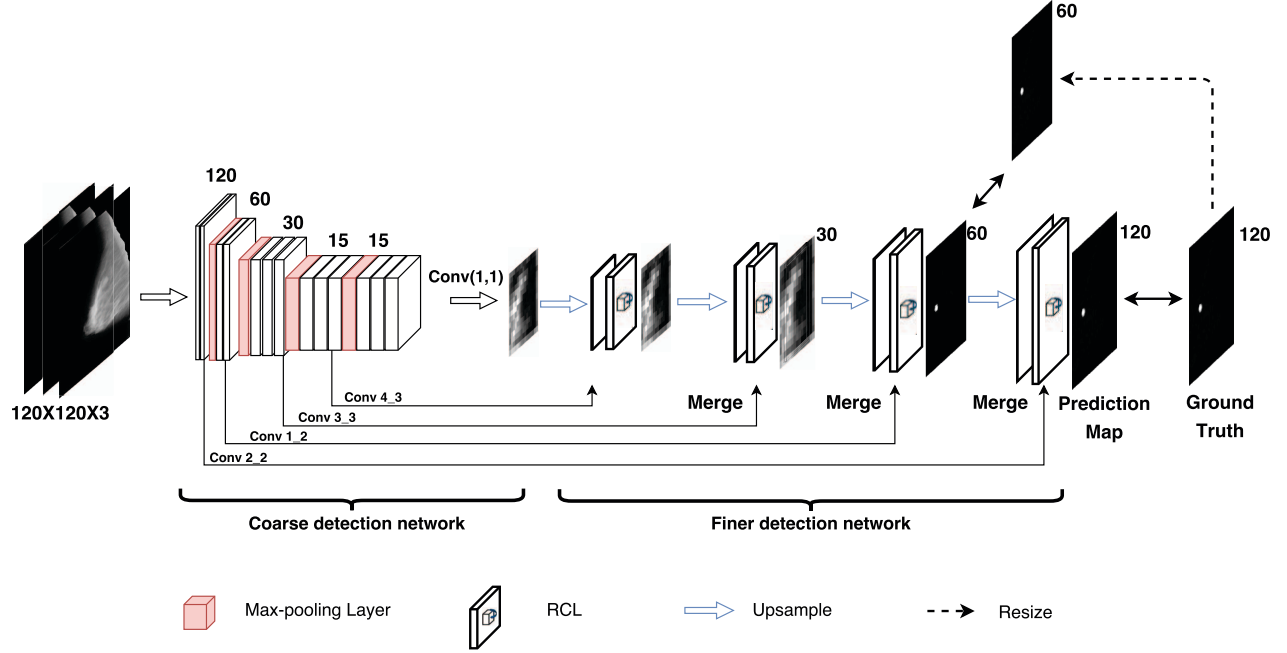


Fig. 3: Fully convolutional deep hierarchical saliency network (FCDHSNet) for suspicious region detection within breast mammogram. Size of the prediction maps along with the spatial dimensions of each feature map are shown.

fully connected networks to have better mixing of higher level features. To simulate non-linearity and to avoid overfitting during learning, we have used ReLU activation function and Dropout layers respectively. We trained our network on DDSM and INbreast databases. The details of the selection of number of training and testing images are described in Table I. During the training of this network we used *categorical cross entropy* as the objective function and learning rate, momentum are initialized at 0.001 and 0.7 respectively. Learning rate was updated by 0.1 times when the training accuracy stopped improving with the current learning rate.

### C. Mass classification

Mass/no-mass decision network outputs whether the suspicious regions have abnormal mass in it. Then, another CNN with the same architecture as in the Table II with intensity features in conjunction with two dimensional discrete wavelet features is trained for benign/malignant mass classification.

Same learning strategy as the mass/no-mass detection network has been followed here as both of them are binary classifiers. Only during training, the trainable parameters are tuned in such a way that both network (same) give multi-tasking capability.

## III. EXPERIMENTS AND RESULTS

### A. Database

We validated the proposed automated framework using publicly available database i.e., CBIS-DDSM database [28] and INbreast [29]. CBIS-DDSM database is the curated version of Digital Database for Screening Mammography (DDSM). Throughout the paper, we have used 'DDSM' for referring to 'CBIS-DDSM'. The data were divided into training and testing sets according to the BI-RADS (Breast Imaging-Reporting and Data System) category. BI-RADS allows an appropriate arrangement for researchers working on CADs. Within 2620 scanned cases based on the magnitude of abnormality, the

TABLE I: Number of training and testing images

Stage	Database	Total images for training	Training images with augmentation	Total images for testing
Mass detection	DDSM	350 (mass present)	$350 \times 9 = 3150$	350 (mass present)
	INbreast	66 (mass present)	$66 \times 9 = 594$	41 (mass present)
Mass/No-mass classification	DDSM	350 (mass) + 466 (no-mass)	$350 \times 4 + 466 \times 3 = 2798$	329 (mass) + 398 (no mass)
	INbreast	66 (mass) + 63 (no-mass)	$66 \times 4 + 63 \times 4 = 516$	39 (mass) + 37 (no-mass)
Benign/Malignant classification	DDSM	160 (Malignant) + 160 (Benign)	$160 \times 4 + 160 \times 4 = 1280$	113 (Benign) + 113 (Malignant)
	INbreast	31 (Malignant) + 33 (Benign)	$31 \times 4 + 33 \times 4 = 256$	20 (Malignant) + 23 (Benign)

TABLE II: Detailed parameters of each layer

Name	Filter size	Depth of Filter	Dropout
Conv1	11	32	
ReLU1	1		
Pooling1	3		
Conv2	11	64	
BatchNorm			
ReLU2	1		
Dropout1			0.5
Pooling2	3		
Conv3	7	96	
ReLU3	1		
Dropout2			0.15
Pooling3	2		
Conv4	5	128	
BatchNorm			
ReLU4	1		
Dropout3			0.25
Pooling4	2		
Fc5	1	5000	
ReLU5	1		
Dropout4			0.5
Fc6	1	1000	
ReLU6	1		
Fc7	1	2	
Softmax	1		

abnormal masses are divided into two classes, benign and malignant. INbreast contains 115 abnormal cases among 410 images, where 68 cases out of 115 have benign findings and 28 cases have malignant findings. We have highlighted the number of images taken on each stage of the whole framework in Table I. All experiments are carried out on a system with the following specification: Intel®Xeon, 3.07GHz CPU with 24GB RAM and graphics card NVIDIA Quadro 6000 6144 MB GDDR5.

### B. Evaluation metrics

To evaluate the performance of our automated framework, we used some of the widely used objective measurement metrics such as F-measure, sensitivity, receiver operating characteristic curve (ROC) and classification accuracy. F-measure and sensitivity are used to evaluate the suspicious region detector's performance while ROC curve is used to evaluate classification performance. Larger values in F-measure and area under the ROC curve stand for good performance. To avoid over-fitting, we trained our network with an equal number of images from each class. For more details on training and testing images, refer Table I.

### C. Suspicious region detection

We have taken a total of 700 abnormal mammograms from the DDSM database (only mediolateral oblique view) to validate our suspicious region detection network. Out of 700 cases, 350 mammograms we have taken for training the FCDHSNet and rest 350 mammograms are for testing. Class of the abnormal masses does not influence the learning of the detection network so, a random selection of 350 cases for training does not affect the prediction quality. As the sensitivity depends on the size of the training set, we have increased our data by augmentation. We took 9 rotations for each training

images ( $[0, 315^\circ]$  with  $45^\circ$  intervals) [30] and increased the training data size 9 times. Fig. 4 and Fig. 5 are shown to highlight different prediction maps by our prediction network from test cases. The network has obtained 0.89 F-measure value after running for 2000 epochs. On the test images, it has shown the sensitivity of 0.94 at 1.13 false positives per image. The detection result is comparable with the current state-of-the-art results (see Table IV). Testing with 350 mammograms results in 329 true positives and 398 false positives. This decision is made by comparing simple euclidean distance between the centroid of all predicted locations and the ground truth.

Detected false positives are reduced by employing another network called mass/no-mass detection. The FCDHSNet predicts the suspicious locations and the mass/no-mass detector eliminates the false positives. False positives per image at different stages are shown in the Table: III and the details of the mass/no-mass detection network are discussed in the subsection: III-E.

TABLE III: Detection performances before and after second stage

Stage	Database	False positive/image
After FCDHSNet	DDSM	1.13
	INbreast	0.96
After mass/no-mass detection network	DDSM	<b>0.024</b>
	INbreast	<b>0.026</b>

### D. Transfer Learning Capability of pre-trained FCDHSNet

This pre-trained FCDHSNet was fine-tuned on INbreast database since it consists of fewer data and might be more prone to over-fitting. As described in the Table: I, we have taken total 594 training images. We fine-tuned the model which obtained 0.94 sensitivity during training. Testing with 41 images results in the sensitivity of 0.96 at 0.96 false positives per image (39 falsely detected regions are generated from 41 test images).

### E. Mass/no-mass detection

We have taken the same 350 mammograms which were chosen during the learning of FCDHSNet. We used a cropping mechanism to segment the abnormal masses as per the provided ground truths. An automated cropping method used the fitted bounding box coordinates to extract suspicious regions from the original mammogram of size  $1024 \times 1024$ . To combine context information, we include 40 pixels more in each direction of the fitted bounding boxes. So, the 350 mass regions and 466 random non-mass tissue regions are used for training. In order to increase training data, we have augmented the mass images by 4 times ( $[0, 270^\circ]$  with  $90^\circ$  intervals) and no-mass tissues by 3 times ( $[0, 180^\circ]$  with  $90^\circ$  intervals). We trained the mass/no-mass classification network with 2798 images and tested it on the predicted regions from the previous detection network. Each of the predicted images

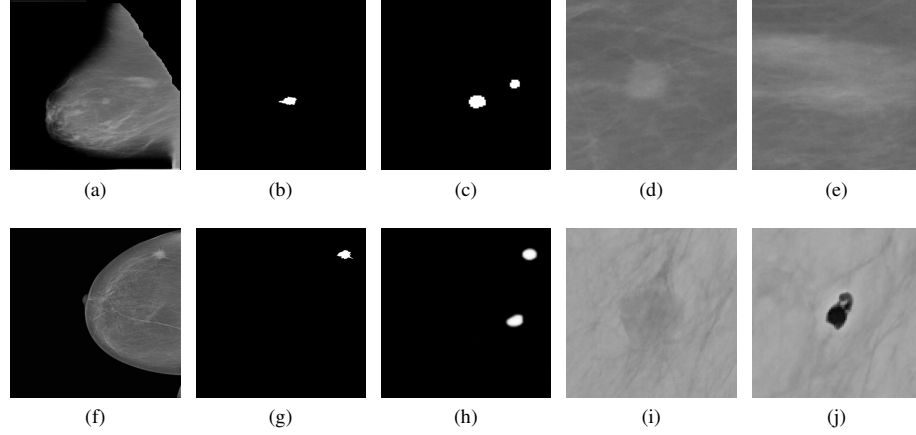


Fig. 4: Suspicious region detection with false positive. (a),(f) Original mammogram (b),(g) Ground truth (c),(h) Predicted map (d),(i) Cropped image containing true positive mass (e),(j) Cropped image containing false positive mass. (a-d) for DDSM & (d-j) for INbreast

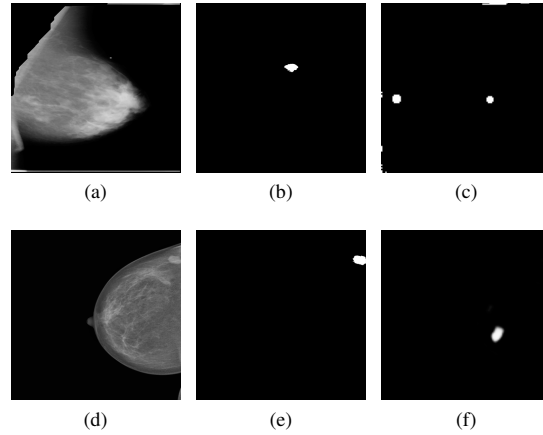


Fig. 5: Mass detection without any true positive (a),(d) Original mammogram (b),(e) Ground truth (c),(f) Predicted map, (a-c) for DDSM & (d-f) for INbreast

is taken as  $84 \times 84 \times 4$  where the first three channels consist of wavelet decomposed sub-images and the last channel is the approximated ROI (refer to II-B) Examples of cropped ROIs which are fed to this network are shown in Fig. 4 and Fig.5.

#### F. Transfer Learning capability of pre-trained classifier

Similar approach is taken for the INbreast database. Instead of training separately, we used the pre-trained model of mass/no-mass classification on DDSM database to fine-tune on INbreast database. The training accuracy of the classification network was 99.24% and 99.58% for DDSM and INbreast databases respectively. We used this pre-trained network to classify between 329 masses, 398 no-masses images in DDSM and 39 masses, 37 no-masses in INbreast. The results are described in Table VI.

#### G. Mass classification

The final stage of the whole framework is to classify the abnormal masses between benign and malignant. We have taken 160 benign cases and 160 malignant cases from DDSM database. An equal number is preferred in order to avoid over-fitting during training. To train this classification network, we again augmented 4 times ( $[0, 270^\circ]$  with  $90^\circ$  intervals) each of the images which results in 1280 training images. The testing is done on the output of mass/no-mass classification network. After getting the abnormal mass labels from the testing images, we pass these mass images to the mass classification network. Testing with the pre-trained classification network shows  $0.9970 \pm 0.0017$  AUC in DDSM and  $0.9977 \pm 0.024$  in Inbreast on ROC curve as in Fig./refResults of the different stages of the proposed network with 5 fold cross validation).

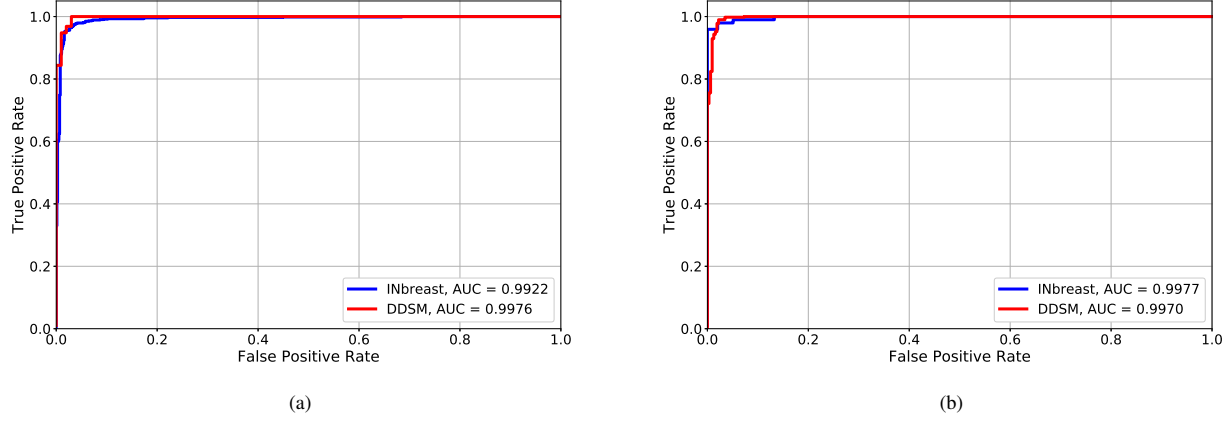


Fig. 6: (a) ROC curve of mass/no-mass classification (b) ROC curve of benign/malignant classification. (Zoom it for better visualization). The model trained on DDSM database has been fine-tuned on INbreast database and the classification performance shows the effectiveness of the transfer-learning.

TABLE IV: Comparison of detection performances

References	Techniques	Database	False positive/image	Sensitivity
Daniilo <i>et al.</i> [31]	Multiple thresholding, GA, DWT	DDSM	1.37	0.95
Daniel <i>et al.</i> [7]	CNN	DDSM	0.9	0.85
Yang <i>et al.</i> [8]	Saliency map, DL	DDSM	3.8	0.93
Dhungel <i>et al.</i> [18]	DL, random forest	DDSM	1.00	0.75
		INbreast	1.2	0.96
Carneiro <i>et al.</i> [14]	Cascaded DL and RF	INbreast	3.67	0.83
M.A. Al-antari <i>et al.</i> [15]	DL based on YOLO	INbreast	X	X
Al-masni <i>et al.</i> [16]	DL based on YOLO	DDSM	0.22	X
<b>DHSNet</b>	Deep hierarchical mass-	DDSM	<b>2.04</b>	<b>0.938</b>
<b>DHSNet</b>	prediction network	INbreast	<b>1.22</b>	<b>0.954</b>
<b>FCDHSNet</b>	Fully-connected Deep hierarchical-	DDSM	<b>1.13</b>	<b>0.94</b>
<b>FCDHSNet</b>	mass prediction network	INbreast	<b>0.96</b>	<b>0.96</b>

TABLE V: Comparison of classification performances

References	Techniques	Database	Classification performance	Uses Ground-Truth ROIs
Xie <i>et al.</i> [32]	Gray level features, textural features	MIAS	96.0%	Yes
Beura <i>et al.</i> [33]	2D-DWT, GLCM	DDSM	95.7%	Yes
		MIAS	98.0%	
Jiao <i>et al.</i> [12]	High & medium level, deep features	DDSM	98.8%	Yes
		DDSM	96.7%	
Arevalo <i>et al.</i> [11]	CNN, SVM	DDSM	96.7%	Yes
Dhungel <i>et al.</i> [9]	Cascaded CNN & RF	INbreast	91%	No
Atlas <i>et al.</i> [10]	SVM, ANN	INbreast	97.5%	Yes
P.R.Sarkar <i>et al.</i> [13]	Segmented ROIs, CNN	DDSM	99.26%	Yes
Carneiro <i>et al.</i> [14]	Cascaded CNN	INbreast	NA%	No
M.A. Al-antari <i>et al.</i> [15]	DL based on YOLO	INbreast	95.64%	No
Al-masni <i>et al.</i> [16]	DL based on YOLO	DDSM	97.00%	No
<b>Ours</b>	<b>2D-DWT, CNN</b>	DDSM	<b>98.05%</b>	No
<b>Ours</b>	<b>2D-DWT, CNN</b>	INbreast	<b>98.14%</b>	No



TABLE VI: Results of the different stages of the proposed network with 5 fold cross validation

Stage	Database	Metrics during training	Metrics during testing
Mass detection	DDSM	F-measure = 0.89	Sensitivity = 0.94
	INbreast	F-measure = 0.92	Sensitivity = 0.96
Mass/No-mass classification	DDSM	Accuracy = 0.9924	Accuracy = $0.9802 \pm 0.0015$ Sensitivity = $0.9701 \pm 0.0029$ Specificity = $0.9887 \pm 0.0014$
	INbreast	Accuracy = 0.9958	Accuracy = $0.9816 \pm 0.012$ Sensitivity = $0.9749 \pm 0.017$ Specificity = $0.9892 \pm 0.014$
Benign/Malignant classification	DDSM	Accuracy = 0.9911	Accuracy = $0.9805 \pm 0.0051$ Sensitivity = $0.9755 \pm 0.0072$ Specificity = $0.9857 \pm 0.0048$
	INbreast	Accuracy = 0.9853	Accuracy = $0.9814 \pm 0.0194$ Sensitivity = $0.9805 \pm 0.0267$ Specificity = $0.9829 \pm 0.0233$

#### IV. DISCUSSION

We have compared the performance of the proposed automated framework with the methods presented in the literature. The work discussed in literature used a multiple number of features and usage of multiple low or middle-level features limits the performance. While the use of deep features adds more high-level meaning of the data. FCDHSNet, the detection network simulates the recurrent connections of our brain and it analyses the mammograms hierarchically and progressively. This deep network helps to learn the optimal conditions of various complex parameters like shapes, size, appearances, compactness, and their optimal combination. We used three channel inputs to highlight the dense locations along with the masses and expected the network to learn from the global contrast too. The sensitivity of 0.94 in DDSM and 0.96 in INbreast database, mass detection network outperformed the reported state-of-the-art results.

Similarly, in the classification task, we used both the spectral and spatial features by extracting deep features from the wavelet decomposed sub-images along with the approximated ROI. Here, we show that we can use CNN to learn embedded patterns from the complex features. The fourth channel (refer II-B) includes an approximation of the cropped mass region which also includes intensity information. Final classification performance between benign and malignant mass also outperformed the state-of-the-arts. It has to be noted that all the accuracies reported so far have considered ground truth saliency regions. Although the improvement of our approach in both data sets looks marginal, it is in addition to its generalization capability. In Table V comparison of classification performances are highlighted.

We have compared the overall-classification performance between the proposed method which works on Daubechies two dimensional Discrete Wavelet Transform (2D-DWT) of images

and the method which has the same architecture but works on the raw images. Third column of Table VII shows the clear improvement in classification performance. The fourth column shows the time taken by the proposed network to train one image. It is evident that the RAW image takes less time to train which is because of single channel data where 2D-DWT requires four channels of input data.

TABLE VII: Comparison between overall classification performances and training time between proposed framework with RAW image and 2D-DWT as input.

Method	Database	Accuracy at the final stage	Training time (sec/image)
with RAW image	DDSM	93.31	0.113
	INbreast	95.065	0.102
with 2D-DWT	DDSM	98.05	0.135
	INbreast	98.14	0.119

#### V. CONCLUSION AND FUTURE WORKS

In this paper, we present an automated breast mass classification CAD system which includes suspicious regions identification in mammograms, classification of mass/no-mass and classification between benign or malignant. Our mass detection network is computationally efficient and provides the best result among all the methods reported so far. The decision of mass or no-mass on the predicted map from the detection network is taken by fusing spectral and spatial features. Classification of the masses is done using the same network as the mass/no-mass classification network. All the models are pre-trained on augmented training data from the DDSM database and tested on the different cases. Our proposed framework is completely automatic, once the pre-trained models are provided. Unlike the existing methods mentioned here, rotation variant classification is not an issue for our

proposed network. Promising results emphasize to use this framework to help the radiologists during diagnosis procedure.

In the future, we will try to evaluate the model on different imaging modalities with transfer learning. The performance of the whole can be improved with a bigger database where augmentation will not be required to produce synthetic data.

## REFERENCES

- [1] Globocan project 2012. International Agency for Research on Cancer. [Online]. Available: <http://globocan.iarc.fr/>
- [2] R. L. Siegel, K. D. Miller, and A. Jemal, "Cancer statistics, 2017," *CA: A Cancer Journal for Clinicians*, vol. 67, no. 1, pp. 7–30, 2017. [Online]. Available: <http://dx.doi.org/10.3322/caac.21387>
- [3] A. Jalalian, S. B. Mashohor, H. R. Mahmud, M. I. B. Saripan, A. R. B. Ramli, and B. Karasfi, "Computer-aided detection/diagnosis of breast cancer in mammography and ultrasound: a review," *Clinical imaging*, vol. 37, no. 3, pp. 420–426, 2013.
- [4] R. A. Castellino, "Computer aided detection (cad): an overview," *Cancer Imaging*, vol. 5, no. 1, p. 17, 2005.
- [5] N. Liu and J. Han, "Dhsnet: Deep hierarchical saliency network for salient object detection," in *Proceedings of the IEEE Conference on Computer Vision and Pattern Recognition*, 2016, pp. 678–686.
- [6] Y. LeCun, Y. Bengio, and G. Hinton, "Deep learning," *Nature*, vol. 521, no. 7553, pp. 436–444, 2015.
- [7] M. G. Ertoşun and D. L. Rubin, "Probabilistic visual search for masses within mammography images using deep learning," in *Bioinformatics and Biomedicine (BIBM), 2015 IEEE International Conference on*. IEEE, 2015, pp. 1310–1315.
- [8] Y. Hu, J. Li, and Z. Jiao, "Mammographic mass detection based on saliency with deep features," in *Proceedings of the International Conference on Internet Multimedia Computing and Service*. ACM, 2016, pp. 292–297.
- [9] N. Dhungel, G. Carneiro, and A. P. Bradley, "A deep learning approach for the analysis of masses in mammograms with minimal user intervention," *Medical image analysis*, vol. 37, pp. 114–128, 2017.
- [10] N. El Atlas, A. Bybi, and H. Drissi, "Features fusion for characterizing inbreast-database masses," in *Electrical and Information Technologies (ICEIT), 2016 International Conference on*. IEEE, 2016, pp. 374–379.
- [11] J. Arevalo, F. A. González, R. Ramos-Pollán, J. L. Oliveira, and M. A. G. Lopez, "Convolutional neural networks for mammography mass lesion classification," in *Engineering in Medicine and Biology Society (EMBC), 2015 37th Annual International Conference of the IEEE*. IEEE, 2015, pp. 797–800.
- [12] Z. Jiao, X. Gao, Y. Wang, and J. Li, "A deep feature based framework for breast masses classification," *Neurocomputing*, vol. 197, pp. 221–231, 2016.
- [13] P. R. Sarkar, D. Mishra, and G. R. S. Subrahmanyam, "Classification of breast masses using convolutional neural network as feature extractor and classifier," in *Proceedings of 2nd International Conference on Computer Vision & Image Processing*. Springer, 2018, pp. 25–36.
- [14] G. Carneiro, J. Nascimento, and A. P. Bradley, "Automated analysis of unregistered multi-view mammograms with deep learning," *IEEE transactions on medical imaging*, vol. 36, no. 11, pp. 2355–2365, 2017.
- [15] M. A. Al-antari, M. A. Al-masni, M.-T. Choi, S.-M. Han, and T.-S. Kim, "A fully integrated computer-aided diagnosis system for digital x-ray mammograms via deep learning detection, segmentation, and classification," *International Journal of Medical Informatics*, vol. 117, pp. 44–54, 2018.
- [16] M. A. Al-masni, M. A. Al-antari, J.-M. Park, G. Gi, T.-Y. Kim, P. Rivera, E. Valarezo, M.-T. Choi, S.-M. Han, and T.-S. Kim, "Simultaneous detection and classification of breast masses in digital mammograms via a deep learning yolo-based cad system," *Computer methods and programs in biomedicine*, vol. 157, pp. 85–94, 2018.
- [17] J. Redmon, S. Divvala, R. Girshick, and A. Farhadi, "You only look once: Unified, real-time object detection," in *Proceedings of the IEEE conference on computer vision and pattern recognition*, 2016, pp. 779–788.
- [18] N. Dhungel, G. Carneiro, and A. P. Bradley, "Automated mass detection in mammograms using cascaded deep learning and random forests," in *Digital Image Computing: Techniques and Applications (DICTA), 2015 International Conference on*. IEEE, 2015, pp. 1–8.
- [19] J. Yosinski, J. Clune, Y. Bengio, and H. Lipson, "How transferable are features in deep neural networks?" in *Advances in neural information processing systems*, 2014, pp. 3320–3328.
- [20] R. M. Rangayyan, L. Shen, Y. Shen, J. L. Desautels, H. Bryant, T. J. Terry, N. Horeczko, and M. S. Rose, "Improvement of sensitivity of breast cancer diagnosis with adaptive neighborhood contrast enhancement of mammograms," *IEEE transactions on information technology in biomedicine*, vol. 1, no. 3, pp. 161–170, 1997.
- [21] E. D. Pisano, S. Zong, B. M. Hemminger, M. DeLuca, R. E. Johnston, K. Muller, M. P. Braeuning, and S. M. Pizer, "Contrast limited adaptive histogram equalization image processing to improve the detection of simulated spiculations in dense mammograms," *Journal of Digital Imaging*, vol. 11, no. 4, pp. 193–200, 1998.
- [22] K. Zuiderveld, "Contrast limited adaptive histogram equalization," P. S. Heckbert, Ed. San Diego, CA, USA: Academic Press Professional, Inc., 1994, ch. Contrast limited adaptive histogram equalization, pp. 474–485. [Online]. Available: <http://portal.acm.org/citation.cfm?id=180940>
- [23] X. Bai and F. Zhou, "Multi scale top-hat transform based algorithm for image enhancement," in *Signal Processing (ICSP), 2010 IEEE 10th International Conference on*. IEEE, 2010, pp. 797–800.
- [24] K. Simonyan and A. Zisserman, "Very deep convolutional networks for large-scale image recognition," *arXiv preprint arXiv:1409.1556*, 2014.
- [25] M. Liang and X. Hu, "Recurrent convolutional neural network for object recognition," in *Proceedings of the IEEE Conference on Computer Vision and Pattern Recognition*, 2015, pp. 3367–3375.
- [26] M. M. Jadoon, Q. Zhang, I. U. Haq, S. Butt, and A. Jadoon, "Three-class mammogram classification based on descriptive cnn features," *BioMed research international*, vol. 2017, 2017.
- [27] I. Daubechies, *Ten lectures on wavelets*. SIAM, 1992.
- [28] A. H. Rebecca Sawyer Lee, Francisco Gimenez and D. Rubin, "Curated breast imaging subset of ddsn," 2016. [Online]. Available: <http://dx.doi.org/10.7937/K9/TCIA.2016.7002S9CY>
- [29] I. C. Moreira, I. Amaral, I. Domingues, A. Cardoso, M. J. Cardoso, and J. S. Cardoso, "Inbreast: toward a full-field digital mammographic database," *Academic radiology*, vol. 19, no. 2, pp. 236–248, 2012.
- [30] H. R. Roth, L. Lu, J. Liu, J. Yao, A. Seff, K. Cherry, L. Kim, and R. M. Summers, "Improving computer-aided detection using convolutional neural networks and random view aggregation," *IEEE transactions on medical imaging*, vol. 35, no. 5, pp. 1170–1181, 2016.
- [31] D. C. Pereira, R. P. Ramos, and M. Z. Do Nascimento, "Segmentation and detection of breast cancer in mammograms combining wavelet analysis and genetic algorithm," *Computer methods and programs in biomedicine*, vol. 114, no. 1, pp. 88–101, 2014.
- [32] W. Xie, Y. Li, and Y. Ma, "Breast mass classification in digital mammography based on extreme learning machine," *Neurocomputing*, vol. 173, pp. 930–941, 2016.
- [33] S. Beura, B. Majhi, and R. Dash, "Mammogram classification using two dimensional discrete wavelet transform and gray-level co-occurrence matrix for detection of breast cancer," *Neurocomputing*, vol. 154, pp. 1–14, 2015. [Online]. Available: <http://www.sciencedirect.com/science/article/pii/S0925231214016968>